Journal Name

ARTICLE

Supporting Information

Received 00th January 20xx,
Accepted 00th January 20xx

DOI: 10.1039/x0xx00000x

www.rsc.org/

σ-Hammett Parameter: a Strategy to Enhance Both Photo- and Electro-luminescence Features of Heteroleptic Copper(I) Complexes

Michael D. Weber,[a] Marta Viciano-Chumillas,[b*] Donatella Armentano,[c] Joan Cano,[b,d] and Rubén D.

[a] *M. D. Weber and Dr. R. D. Costa*
Department of Chemistry and Pharmacy
University of Erlangen-Nuremberg (FAU)
Egerlandstr. 3, D-91058 Erlangen, Germany.
E-mail: ruben.costa@fau.de
[b] *Dr. M. Viciano-Chumillas and Dr. J. Cano*
Institut de Ciència Molecular (ICMol)
Universitat de València, 46980 Paterna, València, Spain.
E-mail: marta.viciano@uv.es
[c] *Dr. D. Armentano*
Dipartamento di Chimica e Tecnologie Chimiche (CTC), Università della Calabria, 87030 Rende, Cosenza, Italy
[d] *Dr. J. Cano*
Fundació General de la Universitat de València (FGUV)
Universitat de València, 46980 Paterna, València, Spain

Costa[a*]

Table S1. Crystal data for **1**–**4.**

	$C_{51}H_{44}CuN_2O_3P_2{\cdot}BF_4{\cdot}C_4H_{10}O{\cdot}CH_2Cl_2$ (**1**)	$C_{51}H_{44}CuN_2OP_2{\cdot}BF_4$ (**2**)	$C_{49}H_{40}CuN_2OP_2{\cdot}BF_4$ (**3**)	$C_{49}H_{38}CuN_4O_5P_2{\cdot}BF_4{\cdot}CH_2Cl_2$ (**4**)
Formula weight [gmol^{-1}]	1104.23	913.18	885.134	1060.06
Crystal system	Triclinic	Triclinic	Monoclinic	Monoclinic
Space group	*P*–1	*P*–1	$P2_1/n$	$P2_1/c$
a [Å]	10.3039(8)	11.5671(5)	10.5556(8)	13.4559(4)
b [Å]	14.7177(12)	12.8076(16)	21.7911(16)	19.0621(6)
c [Å]	18.7453(14)	16.809(2)	19.1037(14)	18.7780(6)
α [º]	74.574(3)	80.990(6)	90	90
β [º]	87.910(3)	72.435(6)	96.636(4)	101.7046(11)
γ [º]	74.470(3)	71.587(6)	90	90
V [Å^3]	2638.4(4)	2247.4(5)	4364.8(6)	4716.4(3)
Z	2	2	4	4
D_{calc} [gcm^{-3}]	1.390	1.349	1.347	1.493
Number of collected reflections (unique)	37850(10728)	118835(11920)	187774(7391)	80070(8244)
Number of observed reflections ($I_o > 2\sigma(I_o)$)	8578	9678	6437	7079
Internal R factor	0.057	0.038	0.054	0.034
Number of parameters	656	560	541	622
Goodness-of-fit S on F^2	0.85	0.96	1.04	0.69
Largest peak and hole in final difference Fourier map (e Å^{-3})	−1.25 and 1.98	−0.46 and 0.82	−0.48 and 1.31	−0.90 and 1.54
μ [mm^{-1}]	0.638	0.614	0.630	0.713
R_1[a] [I> 2.0σ(I)]	0.0680	0.0450	0.0445	0.0351
wR_2[b] [all data]	0.2132	0.1742	0.1480	0.1133
T [K]	90	296	296	90

[a] $R_1 = \sum||F_o| - |F_c|| / \sum|F_o|$. [b] $wR_2 = \{\sum[w(F_o^2-F_c^2)^2]/\sum w(F_o^2)^2\}^{1/2}$.

Table S2. Selected bond lengths (Å) and angles (º) for compounds [Cu(Xantphos)(R_2bipy)]BF_4 (**1–4**).

Compound	1	2	3	4
Bond lengths				
Cu–P1	2.2460(10)	2.2816(6)	2.2734(8)	2.2677(7)
Cu–P2	2.2513(10)	2.2429(6)	2.3033(8)	2.2657(7)
Cu–N1	2.073(3)	2.0705(18)	2.136(2)	2.065(2)
Cu–N2	2.023(3)	2.0775(17)	2.078(2)	2.0824(19)
Cu···O1	3.198(2)	3.169(2)	3.082(2)	3.120(2)
P1···P2	3.843	3.913	3.830	3.815
Bond angles				
P1–Cu–P2	117.42(4)	119.72(2)	113.64(3)	114.61(2)
N1–Cu–N2	79.82(12)	79.86(7)	79.26(9)	79.41(7)
N1–Cu–P1	116.31(9)	110.52(5)	105.13(7)	116.19(6)
N1–Cu–P2	109.86(9)	107.54(5)	117.27(7)	112.89(6)
P1–Cu–N2	112.83(9)	102.45(5)	126.65(7)	123.61(6)
P2–Cu–N2	114.93(9)	129.17(5)	110.30(7)	105.77(6)

Table S3. Details (distances [Å] and angles [º]) of the π···π interactions in [Cu(Xantphos)(R_2bipy)]BF_4 (**1–4**).

Compound	Cg···Cg[a]	Cg···Cg	α[b]
1	Cg8···Cg10 intram	3.855(2)	9.51(18)
2	Cg4···Cg4	3.9025(14)	0.00(11)
2	Cg4···Cg7 intram	3.985(3)	27.3(2)
3	Cg8···Cg10 intram	3.957(2)	30.01(17)
4	Cg8···Cg10 intram	3.6790(15)	14.83(13)

[a] Cg are the six-membered rings: Cg4, N2, C45–C49; Cg7, C16–C21; Cg8, C22–C27; Cg10, C34–C39. [b] α is the dihedral angle between each pair of mean ring planes.

Table S4. Dihedral angle between CuN_2 and CuP_2 planes (θ) of **1**–**4** at the optimized gas geometries.

Compound	S_0	S_1	T_0	oxidized
1	89.34	56.41	59.10	57.92
2	89.50	56.27	59.31	58.60
3	89.48	55.62	58.89	57.98
4	88.41	52.71	57.37	57.90

Table S5. A selection of experimental and theoretical electronic transitions in the UV-Vis region of **1–4**. Wavelengths (λ) and oscillator strengths (f) are in nm and x, respectively.

Compound	λ (gas-gas)[a,b]	λ (gas-solv)[a,c]	λ (solv-solv)[a,d]	λ_{exp}[e]
1	[2] 343 (0.1046)	[2] 324 (0.1406)	[2] 324 (0.1440)	372
	[7] 268 (0.0599)	[7] 256 (0.0652)	[7] 257 (0.0642)	
	[20] 231 (0.2628)	[11] 243 (0.1540)	[11] 244 (0.1273)	285
2	[2] 347 (0.1088)	[2] 325 (0.1405)	[2] 324 (0.1427)	376
	[9] 258 (0.0455)	[4] 270 (0.0299)	[5] 269 (0.0281)	
	[11] 248 (0.1596)	[7] 258 (0.1363)	[8] 257 (0.1990)	281
3	[2] 353 (0.0962)	[2] 328 (0.1227)	[2] 329 (0.1258)	384
	[8] 272 (0.0233)	[5] 272 (0.0280)	[5] 274 (0.0256)	
	[12] 251 (0.2157)	[8] 258 (0.1872)	[8] 258 (0.1926)	282
4	[2] 430 (0.1259)	[2] 418 (0.1531)	[2] 419 (0.1654)	503
	[6] 356 (0.0369)	[4] 362 (0.0451)	[4] 360 (0.0558)	423

[a] Number of the electronic excitation (bracket), wavelength (in nm), and oscillator strength (f x 10^4, parentheses). [b] Geometries optimized and TDDFT in gas phase. [c] Geometries optimized in gas phase and TDDFT using a solvation model. [d] Geometries optimized and TDDFT using a solvation model. [b] Wavelengths (in nm) found from a deconvolution of the experimental spectra.

Table S6. Relative energies (in eV) of the S_0, S_1 and T_0 states of **1–4** in the optimized geometries (in gas phase) for each state and wavelengths (in nm) of the fluorescence and phosphorescence emission. Results were calculated in gas phase and using a solvation model with the parameters for the acetonitrile solvent.

Compound		S_0 (eV) [a]	S_1 (eV) [b]	T_0 (eV) [c]	T_0' (eV) [d]	Fluor. [e]	Phosphor. [f]
			Solvation model				
1	S_0	0.00	0.77	0.78	0.80	623	719 (904)
	T_0	3.12	2.56	2.51	2.52		
	S_1	3.46	2.76	2.81	2.79		
2	S_0	0.00	0.76	0.76	0.78	636	742 (913)
	T_0	3.02	2.49	2.44	2.44		
	S_1	3.36	2.71	2.76	2.74		
3	S_0	0.00	0.76	0.76	0.75	653	768 (940)
	T_0	3.03	2.44	2.17	2.38		
	S_1	3.31	2.66	2.55	2.72		
4	S_0	0.00	0.72	---	0.69	926	1193 (1660)
	T_0	2.39	1.84	---	1.73		
	S_1	2.67	2.06	---	2.13		
			Gas phase				
1	S_0	0.00	0.74	0.75	0.77	675	791 (873)
	T_0	3.10	2.38	2.33	2.34		
	S_1	3.32	2.58	2.65	2.63		
2	S_0	0.00	0.74	0.73	0.75	696	822 (903)
	T_0	2.99	2.29	2.24	2.25		
	S_1	3.21	2.52	2.60	2.56		
3	S_0	0.00	0.74	0.73	0.75	720	859 (936)
	T_0	2.92	2.23	2.17	2.18		
	S_1	3.15	2.46	2.55	2.52		
4	S_0	0.00	0.71	---	0.66	953	1338 (1318)
	T_0	2.43	1.62	---	1.59		
	S_1	2.65	2.01	---	2.11		

[a] Optimized geometry for S_0. [b] Optimized geometry for S_1. [c] Optimized geometry for T_0 using the TDDFT to follow the energy of the T_0 state. [d] Optimized geometry for T_0 where the energy of the state was calculated from a direct calculation on a triplet state. [e] Wavelength (in nm) for the fluorescence emission. [f] Wavelength (in nm) for the phosphorescence emission. In parentheses is shown the value obtained from energies of S_0 and T_0 independently calculated, that is, calculation on singlet and triplet states were done for the S_0 and T_0, respectively.

Table S7. Bond lengths of compounds **1–4** at the optimized gas geometries.

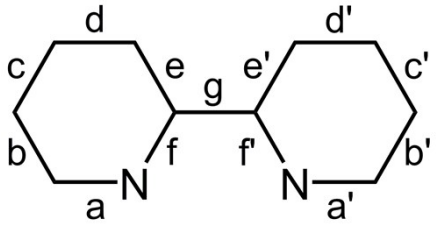

Compound		S_0 [a]	Ox [a]	S_1 [a]	T_0 [a]
1	a	1.352	1.346	1.350	1.362
	b	1.386	1.390	1.380	1.373
	c	1.406	1.404	1.427	1.430
	d	1.402	1.408	1.383	1.380
	e	1.400	1.383	1.419	1.429
	f	1.352	1.365	1.392	1.397
	g	1.489	1.479	1.424	1.416
2	a	1.347	1.347	1.357	1.359
	b	1.392	1.392	1.376	1.376
	c	1.405	1.404	1.432	1.433
	d	1.402	1.406	1.382	1.380
	e	1.400	1.392	1.424	1.425
	f	1.355	1.361	1.386	1.392
	g	1.488	1.478	1.426	1.419
3	a	1.346	1.346	1.361	1.363
	b	1.396	1.394	1.378	1.377
	c	1.398	1.397	1.425	1.428
	d	1.397	1.399	1.378	1.377
	e	1.401	1.395	1.423	1.425
	f	1.356	1.360	1.390	1.396
	g	1.486	1.476	1.427	1.419
4	a	1.346	1.344	1.363	1.365
	b	1.396	1.396	1.379	1.377
	c	1.391	1.388	1.416	1.420
	d	1.390	1.390	1.380	1.378
	e	1.399	1.394	1.407	1.409
	f	1.356	1.358	1.383	1.390
	g	1.483	1.476	1.441	1.431

Table S8. Atomic spin densities (ρ, in electrons) on the C4 and N1 atoms of the R_2bipy ligand and on the copper atom in the T_1 state of **1–4**.

Compound	ρ(Cu)	ρ(C4)	ρ(C4′)	ρ(N1)	ρ(N1′)
1	0.537	0.016	0.006	0.311	0.286
2	0.538	0.066	0.047	0.332	0.328
3	0.537	0.076	0.054	0.345	0.338
4	0.603	0.107	0.057	0.419	0.273

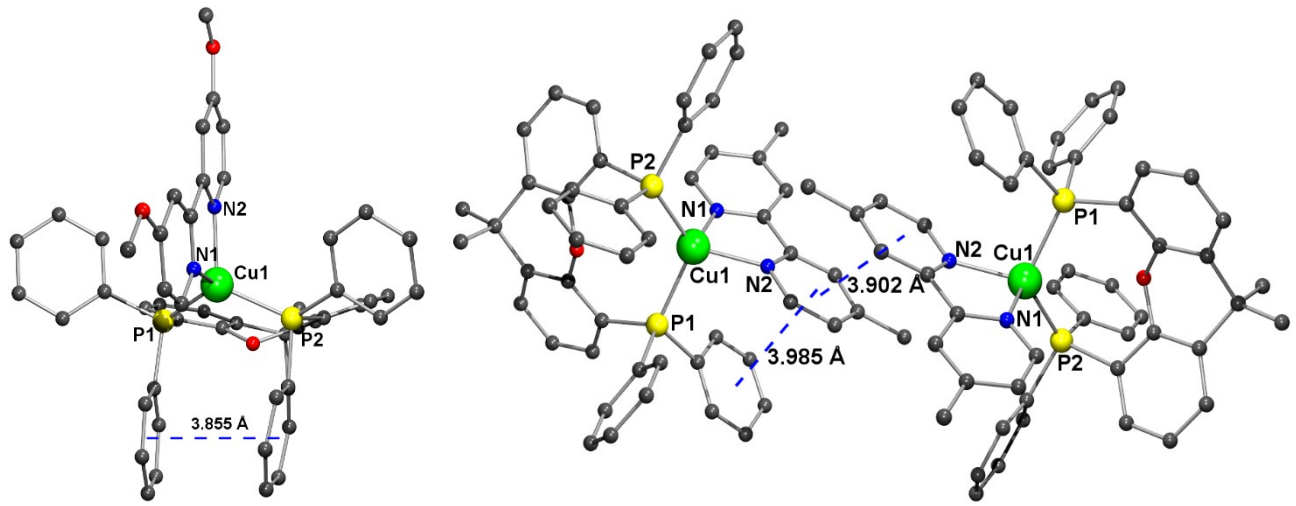

Figure S1. Top: Representation of the intramolecular π–π interaction of **1**. Bottom: Representation of the intra- and inter-molecular π–π interactions of **2**.

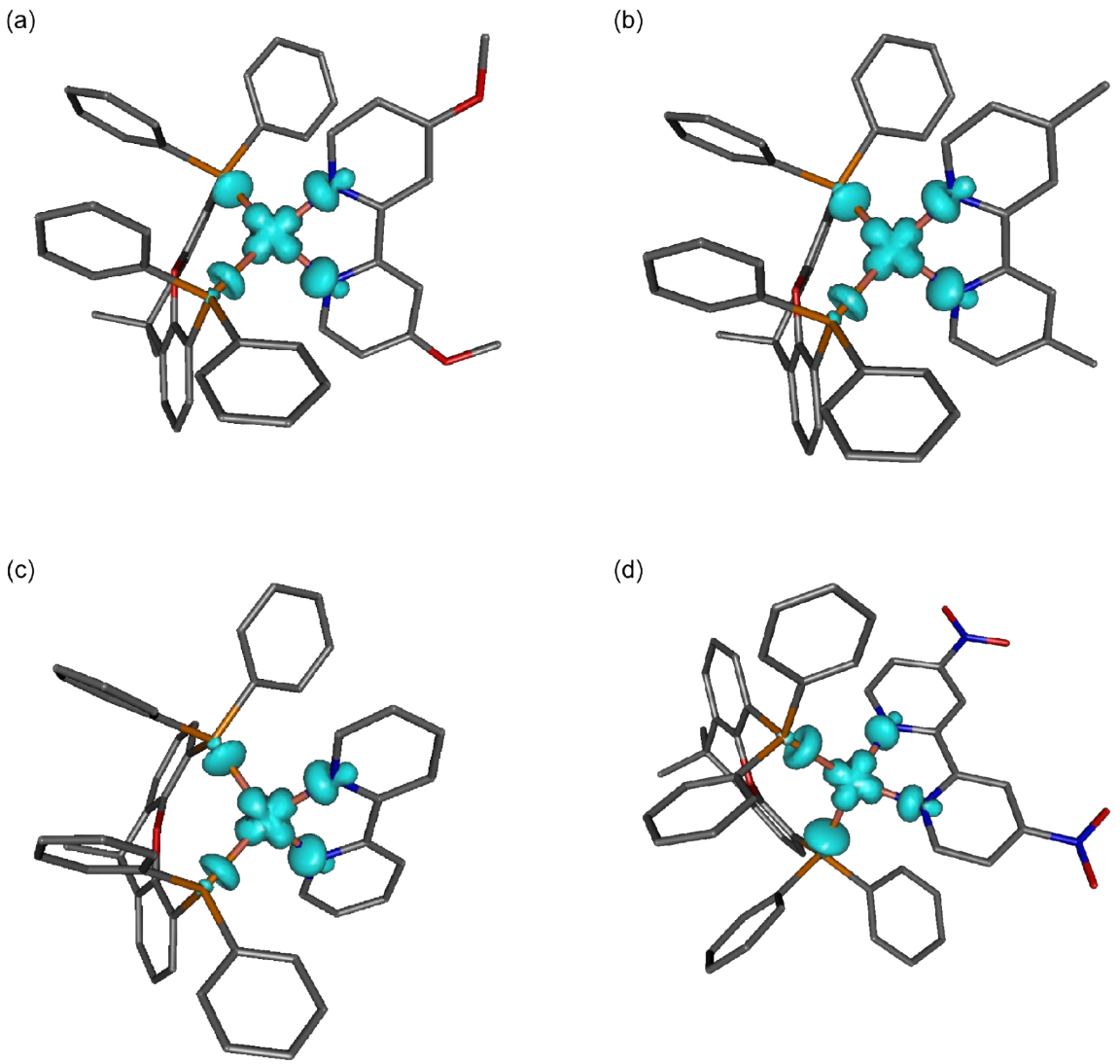

Figure S2. Views of the calculated spin density for the oxidized state of **1–4**. The isodensity surfaces correspond to a cut-off value of 0.005 e bohr^{-3}. Blue and yellow isosurfaces represent the positive and negative regions of spin density, respectively.

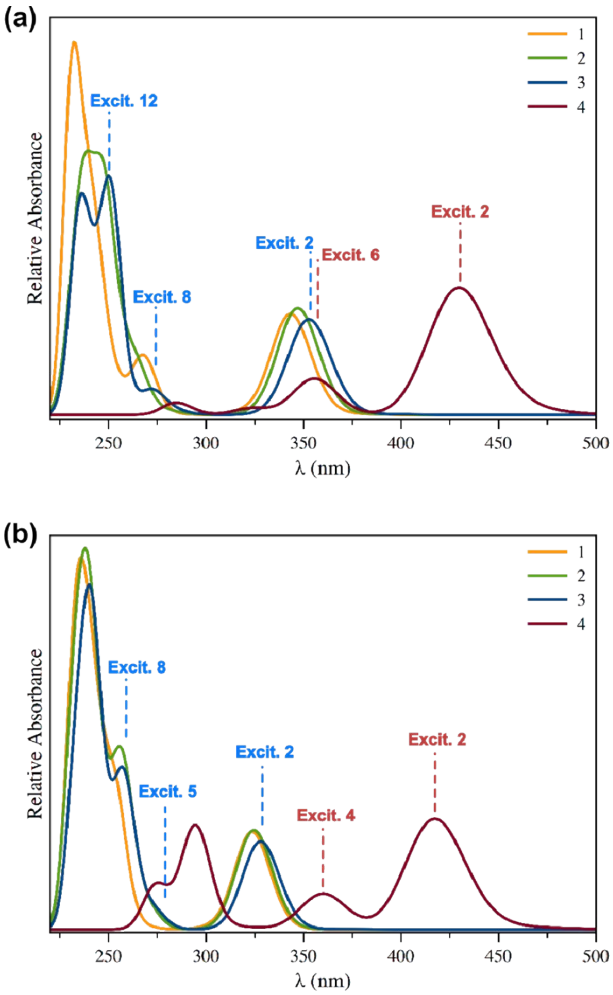

Figure S3. Theoretical absorption spectra for **1–4** simulated from the TDDFT results obtained in (a)-gas phase and (b) using a solvation model. More intense bands of **3** and **4**, which correspond to the electronic transitions shown in Table S5, are marked with a short dashed line in blue and deep red, respectively. Theoretical electronic spectra were simulated using a values for the band-width at half-height of 2000 cm^{-1}.

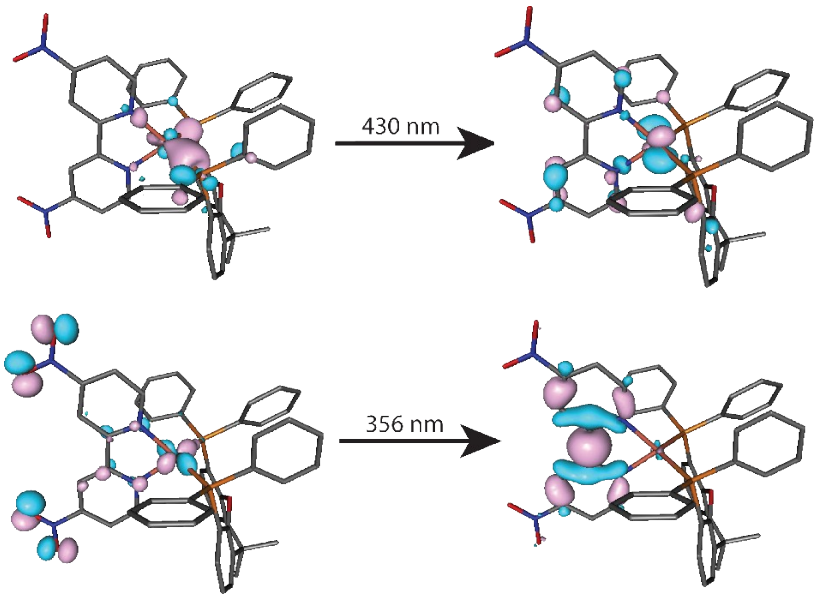

Figure S4. Perspective views of the natural transition orbitals (NTOs) involved in the theoretical electronic excitations of **4**. These trasitions and their correspondence with the experimental absorption spectra are shown in Table S4. The isodensity surfaces correspond to a cut-off value of 0.05 e bohr^{-3}. In the picture, one electron is promoted from the orbital at the left side to the other one at the right side. The wavelenghts for each transitions are those found from a TDDFT calculation in gas phase.

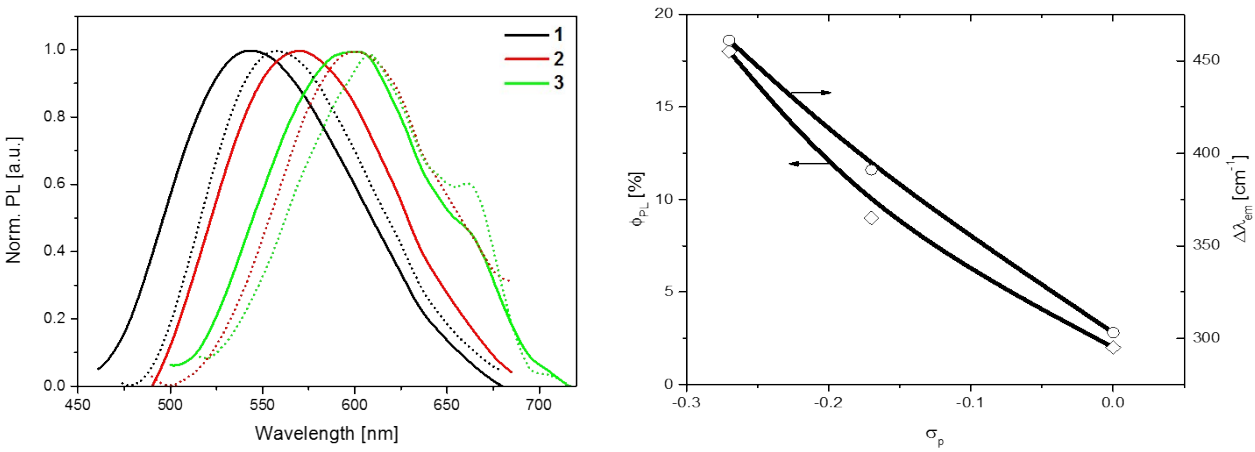

Figure S5. Left: Photoluminescence studies at room temperature (solid line) and 77 K (dotted line) for compounds **1–3** in powder. Right: Photoluminescence quantum yield (left axis) and energy red-shift of the PL from 77K to 293K (right axis) as a function of σ_p.

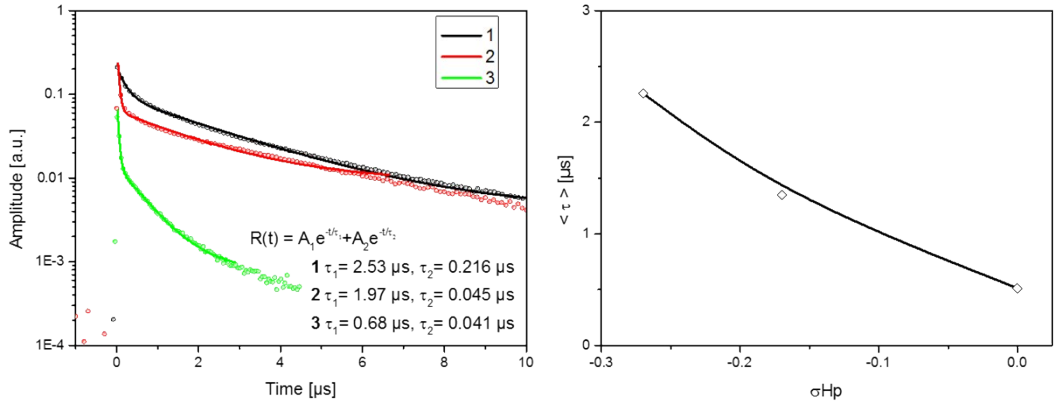

Figure S6. Left: decay profile (symbol) and biexponential fit (solid line) of **1–3**. Right: Average emission lifetimes < τ > of **1–3** as a function of σ_p. The average lifetime can be obtained by using the following formula reported elsewhere:[1]

$$R(t) = \sum_{i=1}^{2} A_i e^{-t/\tau_i}$$

where A_i is constant. The average lifetime can be obtained with:

$$<\tau> = \frac{A_1\tau_1^2 + A_2\tau_2^2}{A_1\tau_1 + A_2\tau_2}$$

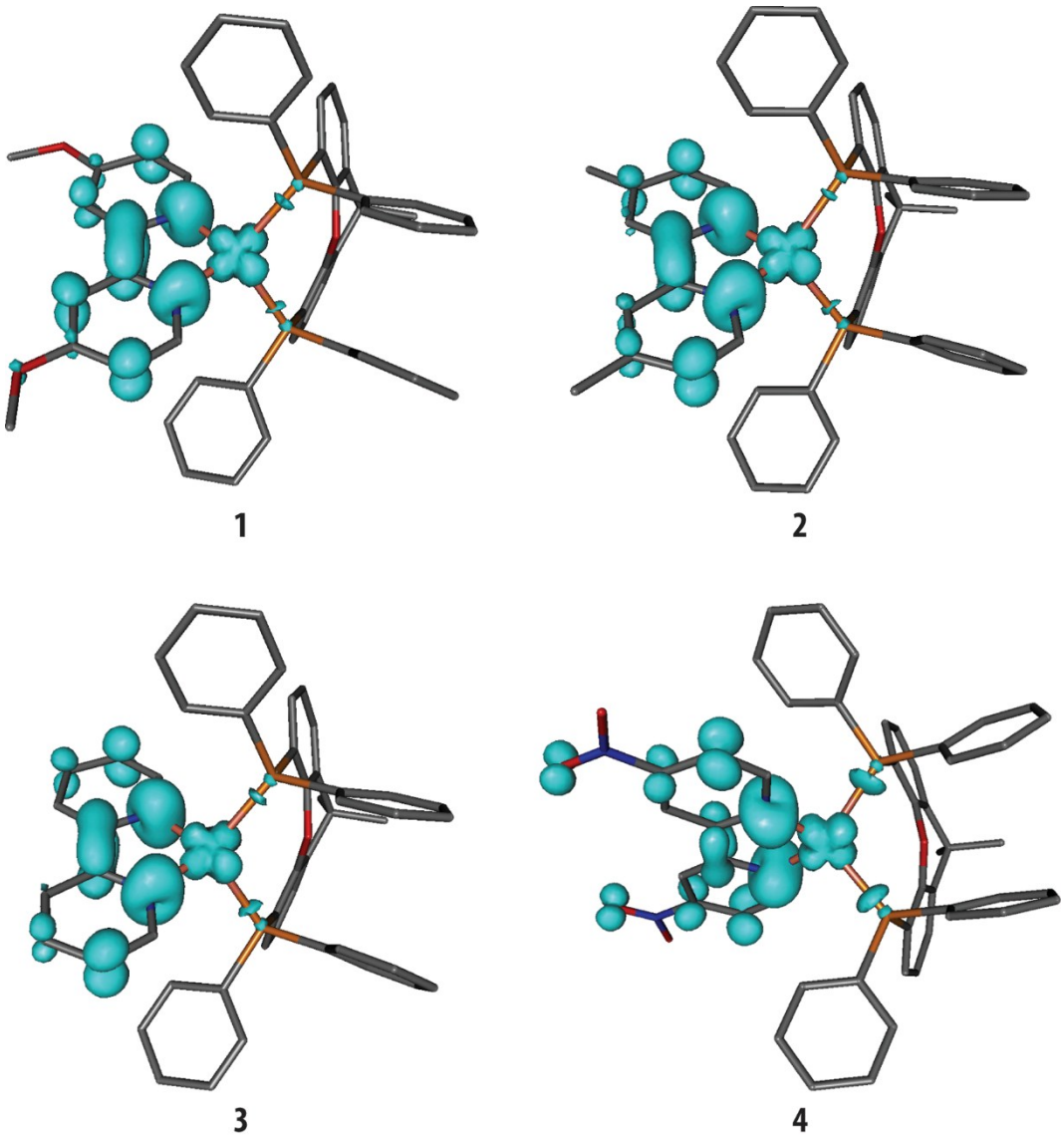

Figure S7. Views of the calculated spin density for the excited T_1 state of **1–4**. The isodensity surfaces correspond to a cut-off value of 0.005 e bohr^{-3}. Blue and yellow isosurfaces represent the positive and negative regions of spin density, respectively.

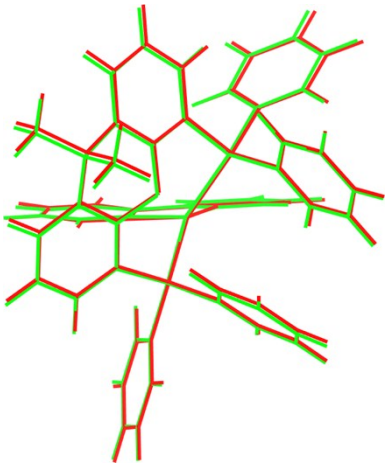

Figure S8. View of the optimized geometries of the S_1 (red) and T_1 (green) state of the $[Cu(Xantphos)(R_2bipy)]^+$ cation of **3**.

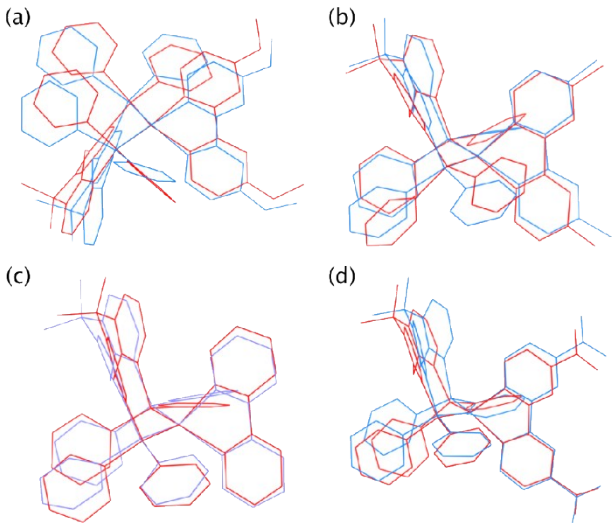

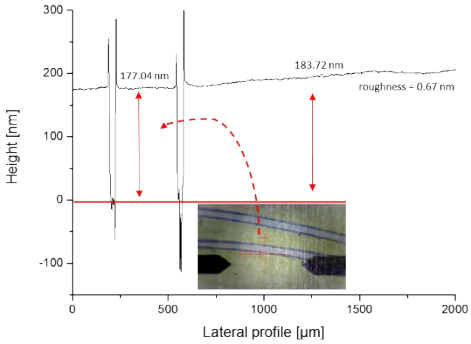

Figure S9. View of the experimental (red) and optimized (blue) geometries of the $[Cu(Xantphos)(R_2bipy)]^+$ cations of **1–4**. The hydrogen atoms were hidden for clarity.

Figure S10. Exemplary profile of a full device (PEDOT:PSS and the active layer) resulting from thickness measurements *via* profilometry technique (zero marked as red line) . Inset: Optical image of the device surface showing the measured scratches as well as the tip of the profilometer and its shadow.

REFERENCES

1 C. M. Luk, L. B. Tang, W. F. Zhang, S. F. Yu, K. S. Teng, S. P. Lau, *J. Mater. Chem.*, **2012**, 22, 22378.